

## PLANETARY-SCALE CHARACTERISTICS OF MONTHLY MEAN LONG-WAVE RADIATION AND ALBEDO AND SOME YEAR-TO-YEAR VARIATIONS

JAY S. WINSTON

National Environmental Satellite Center, ESSA, Washington, D.C.

## ABSTRACT

Global patterns of monthly averages of outgoing long-wave radiation and albedo as derived from TIROS IV radiometer data for the period February-May 1962 are examined relative to each other and with respect to monthly mean mid-tropospheric flow patterns. It is found that long-wave radiation and albedo are inversely correlated on a broad scale, particularly over ocean and non-desert regions. Both quantities show broadscale relationships to the planetary flow patterns over the Northern Hemisphere, particularly the strength and location of features of the wave patterns and the westerlies. Comparisons of long-wave radiation patterns for the same months of two different years, using data from both TIROS IV and VII, show differences averaging about 5 percent and ranging up to about 30 percent of the monthly averaged values. Over the Northern Hemisphere these radiation differences are related to mid-tropospheric circulation differences. Over the equatorial regions and the Southern Hemisphere, where mid-tropospheric circulations are poorly known, the radiation differences serve as indicators of sizable differences in circulation in the two years. Some of the radiation difference patterns are aligned in a series of zonal bands extending over about 60°-90° of longitude and between middle latitudes of both hemispheres; these suggest interactions between large-scale circulations in the two hemispheres.

## 1. INTRODUCTION

The intermittent accumulation of radiometric data from satellites has become sufficiently large in the past few years to permit some study of long-period variations in the planetary-scale outgoing long-wave radiation and albedo for the earth-atmosphere system. Most long-period studies thus far have concentrated on seasonal averages of the data in the form of world maps and/or overall meridional profiles using data from no more than two years for any of the four seasons [2, 3, 16]. The annual variations of the meridional distributions of zonally averaged values of long- and short-wave radiation have been constructed too from monthly mean values for the first year of TIROS VII measurements [8]. In the present study, characteristics of monthly means of long-wave radiation and albedo for several months from both TIROS IV and VII, including comparisons of the same months in two different years, are examined with the aid of world maps and zonal and meridional profiles at selected latitudes and longitudes. For the TIROS IV data the interrelations of the long-wave radiation and albedo are investigated in some detail. Over the Northern Hemisphere the relationship of the radiation data to the monthly mean planetary flow is investigated. Some of these characteristics of long-period changes in outgoing

long-wave radiation were discernible in studies of medium-scale time averages (i.e., 4 or 5 days) in an earlier study of TIROS II data [18] and a more recent study of TIROS IV data [17], but the longer-period scale is better isolated in the data presented here.

## 2. DERIVATION OF DATA

All radiation data used in this study were measured by the 5-channel, scanning radiometers flown on TIROS IV and VII. Details of these radiometers, their pre- and post-launch characteristics, and the data-processing procedures are given in the radiation data catalogs and users' manuals [10, 11, 12, 13, 14]. The data were processed and mapped by electronic computer from copies of the Final Meteorological Radiation Tapes which contain digitized data from all five channels. Only data from the "single, open mode" of operation were used in this study, because of location uncertainties with the other two modes of operation [10, 11].

Values of outgoing long-wave radiation were derived from intensity values of channel 2 (8-12 $\mu$ ). These were converted to total outgoing long-wave radiative flux by means of relationships derived by Wark et al. [15]. Individual values from this channel were corrected for limb-darkening by applying average corrections derived

empirically by Lienesch and Wark [4] from samples of TIROS IV and VII data.

Planetary albedo was obtained from intensity values of channel 3 (0.2–6 $\mu$ ) of TIROS IV. Each individual intensity value, which had a particular solar zenith angle and a certain satellite-viewing angle, was divided by the intensity of radiation that would be reaching the particular viewed spot from outside the atmosphere, assuming a solar constant of 2.00 ly. min.<sup>-1</sup> In this treatment of the data it has been assumed that the reflecting and scattering properties of the atmosphere and the earth's surface are isotropic so that each value of reflectivity at a given spot is assumed to be representative of reflectivity in all directions and hence represents a value of albedo. Admittedly this is a very simple assumption and a study of angular dependence in these TIROS measurements for cloud cases has been made [9]. Results of this study indicate that relatively small changes in albedo (a few percentage units) would generally result from applying an angular adjustment to the data for cloud cases. Such differences are much smaller than the differences between the average uncorrected albedo data and what are thought to be reasonable values for albedo. Thus even though the isotropic assumption could cause some errors in absolute magnitude, it is unlikely that the patterns of the albedo charts could be noticeably altered by applying an angular law to the data. In order to avoid lower intensities of reflected solar radiation, which could lead to more chance of error, no data with solar zenith angles greater than 60° were used. However, this restricts the data sample, mainly at higher latitudes.

The accuracy of the absolute values of the radiation data are questionable because of calibration and degradation problems. Certain correction factors have been presented by Staff Members, NASA [10, 11, 12, 13, 14]. These have been based largely on studies of "quasi-global" average values and are approximate at best. More detailed examination of daily average TIROS IV radiation values by Rao et al. [7] generally verified the degradation corrections for long-wave radiation presented in [10], but adjustments for the albedo values were found to be quite different. Although marked superiority of the corrections for albedo derived in [7] could not be firmly established, they did appear more reasonable when specific cases were examined. Thus the corrections given by Rao et al. were applied to all the TIROS IV data (both long-wave and albedo) appearing in this study. The degradation corrections presented for TIROS VII long-wave radiation data by Staff Members, NASA [11, 12, 13, 14] are somewhat in doubt, particularly in view of some of the results achieved when the corrections were applied. For example, zonal averages for March-May 1964 using these corrections [2] appear to be too high at all latitudes when compared with the corrected TIROS IV values for the period March-May 1962 [16]. Evidently further study of the degradation question for TIROS VII long-wave data is in order, but, lacking such a study at

this time, no corrections have been applied to the TIROS VII long-wave radiation data shown in this study except where specifically noted.

The monthly averaged radiation data have been obtained from daily composite maps of outgoing long-wave radiation and albedo, which have been prepared at the National Environmental Satellite Center for all days when usable measurements were made by TIROS IV and TIROS VII.<sup>1</sup> These composite maps consist of averages of all TIROS observations in 5° latitude-longitude boxes for all orbital passes acquired in a given daily sequence (i.e., over a period of up to 13 hr.). At middle and higher latitudes (poleward of about latitude 30°) these average values usually consist of data from two or more consecutive passes (about 1½ hours apart); in lower latitudes they are usually from one pass. The number of orbital passes of radiation data acquired each day generally varied between 3 and 8 and even with the maximum number acquired there were several major gaps in the data coverage. All daily composite values which were derived from a sufficient data sample (20 or more observations within the box each day) were used in further temporal and spatial averaging of the data.

Since the local time of observation at a given location gradually changes, there can be some bias toward observations taken at certain local times depending upon the period of averaging. The full orbital-solar cycle was approximately 67 days for TIROS IV and about 75 days for TIROS VII. If the data are averaged over periods of one or more multiples of this cycle there is the opportunity to obtain a reasonable sampling of the radiation over all hours of the day at each location. It was in this manner that House [3] studied the heat budget from Suomi's hemispherical sensors on TIROS IV. However, synoptic variations might not insure that this type of average gives a representative sampling of all hours of the day and furthermore the long time periods involved preclude examination of shorter-term variations in the data. For averages over a monthly period, which is somewhat less than half of the orbital-solar cycle, the data originate from periods encompassing somewhat less than half of the day. These times of the day differ mainly with latitude, depending upon the portion of the orbit from which observations of each locality are made. Thus some areas in a given month have data taken during daytime only, some during nighttime only, and others have a combination of the two. Of course, when both albedo and long-wave radiation charts are shown for a given month it is readily apparent which parts of the long-wave radiation data originate predominantly from daytime or nighttime measurements.

If we presume that diurnal variations in surface temperature and cloudiness are small over oceans, these diurnal biases in the data are most important over land areas, particularly those with large diurnal variations in

<sup>1</sup> At the time of this writing TIROS VII daily composites have been prepared continuously through May 1964.

surface temperature and cloudiness. Since the influences of the daytime maxima in cloudiness and surface temperature tend to oppose each other insofar as long-wave radiation is concerned, the effect would be most pronounced in dry, cloudless areas where diurnal temperature variations are extreme. Thus such areas as the Sahara Desert, the Middle East, Australia, parts of southern Africa, and the southwestern United States and Mexico must be considered as subject to strong diurnal bias in many of the time-averaged radiation data shown here. It is possible that with careful consideration of representative surface observations in many of the land areas with respect to diurnal variation of temperature and cloudiness (amount, type, height of tops), one could devise ways of adjusting the radiation values in these regions to be more representative of the entire 24 hours of the day. However, synoptic variations over the day are also involved, so the problem is quite complicated and can never be completely solved so long as the satellite measures the radiation at only one time of a given day.

Monthly mean 700-mb. height values were obtained from the Extended Forecast Division which prepares them from twice-daily objective analyses of the National Meteorological Center. Geostrophic wind speeds were calculated from the monthly mean 700-mb. height values.

### 3. GLOBAL CHARTS AND ZONAL AND MERIDIONAL PROFILES FOR FEBRUARY-MAY 1962

Geographical distributions of long-wave radiation and albedo over much of the earth between latitudes 50° N. and 55° N. for the months of February-May 1962 are shown in figures 1-4. The analyses cover all regions where there were representative radiation values on at least one-tenth of the days in each period. Over the analyzed areas the number of days with data varied considerably and the regions of lesser data coverage are indicated by the dashed isopleths which are used where data were available for less than one-third of the days.

Also shown in each of these figures are the Northern Hemisphere fields of monthly mean 700-mb. height and geostrophic wind derived therefrom. Furthermore, to aid in some of the comparisons from one month to another, profiles of long-wave radiation and albedo along selected latitude circles and meridians are presented in figures 5-8. For these profiles data were not excluded because of too few days of observation, but a binomial smoother (weights of 1:2:1) was applied to both the latitudinal and longitudinal profiles to eliminate small-scale "noise".

Considering first the very broadscale nature of the radiation patterns in figures 1-4, it is seen that zonally oriented maxima of outgoing radiation and minima of albedo (except over desert regions) were located in the Tropics or subtropics of both the Northern and Southern Hemispheres. Situated between these two was the generally narrow belt of low outgoing radiation and high albedo associated with the intertropical convergence zone.

Toward temperate latitudes in both hemispheres the long-wave radiation values decreased and the albedo increased, with strongest gradients between about latitudes 20° and 50°. Poleward from these regions (as far as the data go) long-wave radiation values were generally low and albedo generally high, and gradients were relatively small. In general it is evident that the patterns of long-wave radiation and albedo exhibit an inverse relationship, except over the pronounced desert regions where high albedo values coincide with high values of outgoing radiation. This indicates that the zones of extensive cloudiness consist of clouds that extend to middle and upper levels of the troposphere, since the long-wave radiation tends to be rather low near the maxima of albedo. These variations with latitude and the relationships between long-wave radiation and albedo have been noted on seasonal mean charts presented elsewhere by the author [16] and in average latitudinal profiles for various time periods by several investigators ([6, 18, 1, 2, 3, 8]).

The zonally oriented character of the long-wave radiation and albedo is clearly seen too in the general resemblance of the various profiles along selected meridians (figs. 7 and 8). However, as the maps and comparisons of these profiles show, there are enough deviations from pure zonality to make overall averages for entire latitude circles unrepresentative in some respects. This is particularly true for the equatorial and subtropical regions. Consider, for example, the low outgoing radiation and high albedo of the intertropical convergence zone. Over Africa, South America, and Indonesia the major cloudiness of the convergence zone (as measured by the radiation patterns) was farther south, broader in latitudinal extent, and/or more intense in these months than the zone over the central and eastern Pacific, the Atlantic, and the Indian Oceans. Thus, the profiles along the equator (figs. 5 and 6) are dominated by three major maxima and minima; i.e., minima of long-wave radiation and maxima of albedo where the intertropical convergence zone was over the equator and maxima of long-wave radiation and minima of albedo where the convergence zone was north of the equator or weak.

Also, although most major axes of maximum or minimum long-wave radiation or albedo were mainly zonally oriented, several of them had significant meridional components of orientation as well. This is seen clearly in the extension of the Indonesian convergence area south-eastward toward the central South Pacific (figs. 1-4) and in the general northwest-southeast orientation of the pronounced zones of maximum outgoing radiation (minimum albedo) in the equatorial and subtropical South Pacific and South Atlantic Oceans.

For the albedo, of course, there were also notable variations along latitude circles in subtropical or tropical regions where virtually cloudfree land and ocean areas coexisted. This was most pronounced for the Atlantic Ocean and the Sahara and Saudi Arabia and the Arabian Sea (figs. 1a, 3a, and 6 at 20° N.).

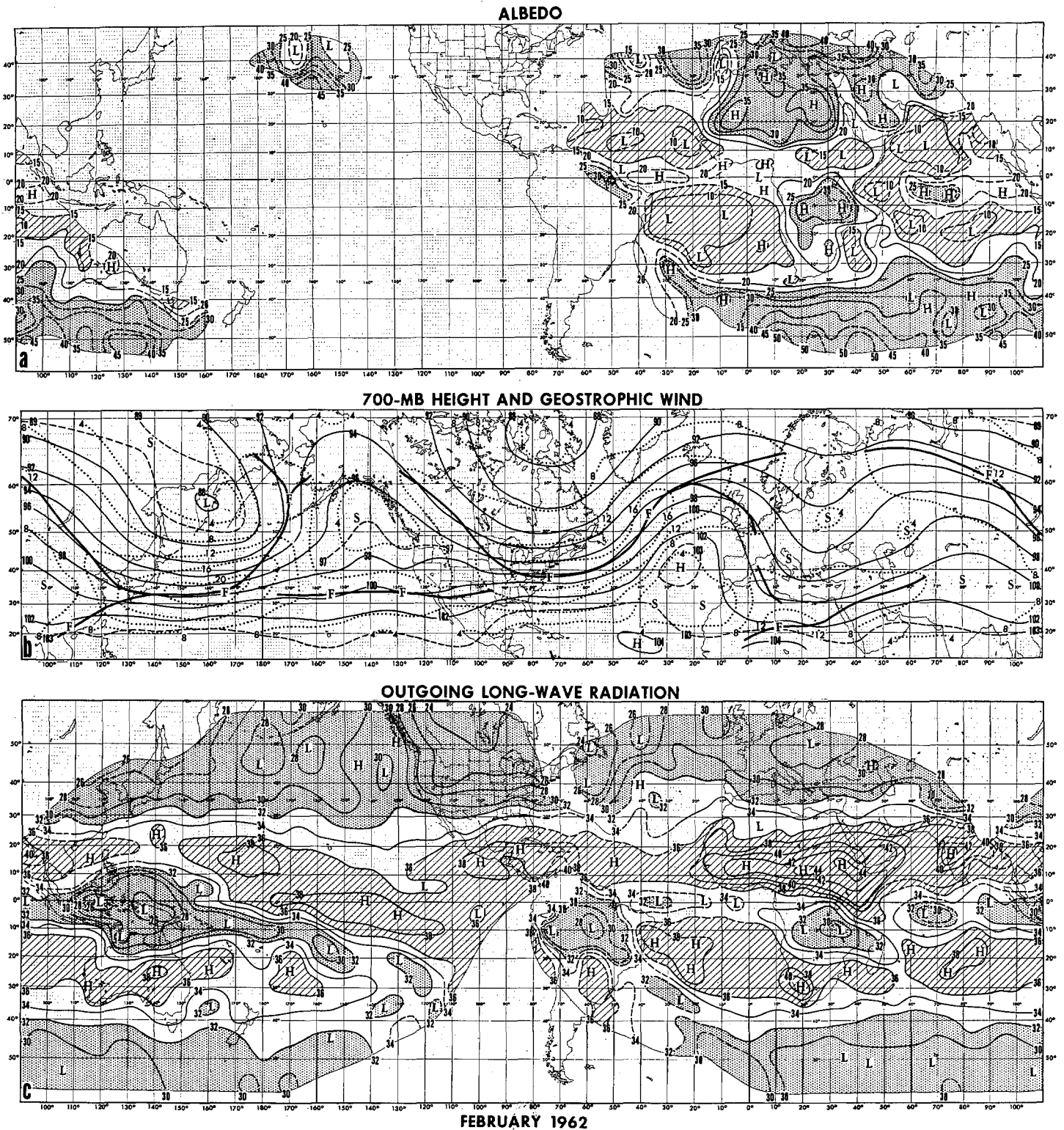


FIGURE 1.—Averages for February 1962 (February 8–28 for radiation data) of (a) Albedo. Isopleths are labeled in percent and are drawn at intervals of 5 percent. Areas with values less than 15 percent are hatched, more than 25 percent, stippled. H and L refer to maxima and minima of albedo, respectively. (b) 700-mb. height and geostrophic wind. Height contours are labeled in 100's of ft. and are drawn at intervals of 200 ft. (solid), with some intermediate 100-ft. contours (dashed). H and L refer to centers of maximum or minimum height, respectively. Isotachs of geostrophic wind speed at 700 mb. (dotted lines) are labeled in m. sec.<sup>-1</sup> and are drawn at intervals of 4 m. sec.<sup>-1</sup>. F and S refer to maxima and minima of wind speed, respectively, except that S is not shown where H and L appear. Well-defined axes of maximum wind speed are indicated by heavy lines where speeds exceed 8 m. sec.<sup>-1</sup> (c) Outgoing long-wave radiation. Isopleths are labeled in hundredths of ly. min.<sup>-1</sup> and are drawn at intervals of  $2 \times 10^{-2}$  ly. min.<sup>-1</sup>. Areas with values less than 0.32 ly. min.<sup>-1</sup> are stippled, more than 0.36 ly. min.<sup>-1</sup>, hatched. H and L refer to maxima and minima of outgoing radiation, respectively. Isopleths in (a) and (c) are dashed in regions with data on less than one-third of the days in the period and no analysis is shown where data were available on less than one-tenth of the days. Data used in (a) and (c) were corrected for instrumental degradation as described in [7].

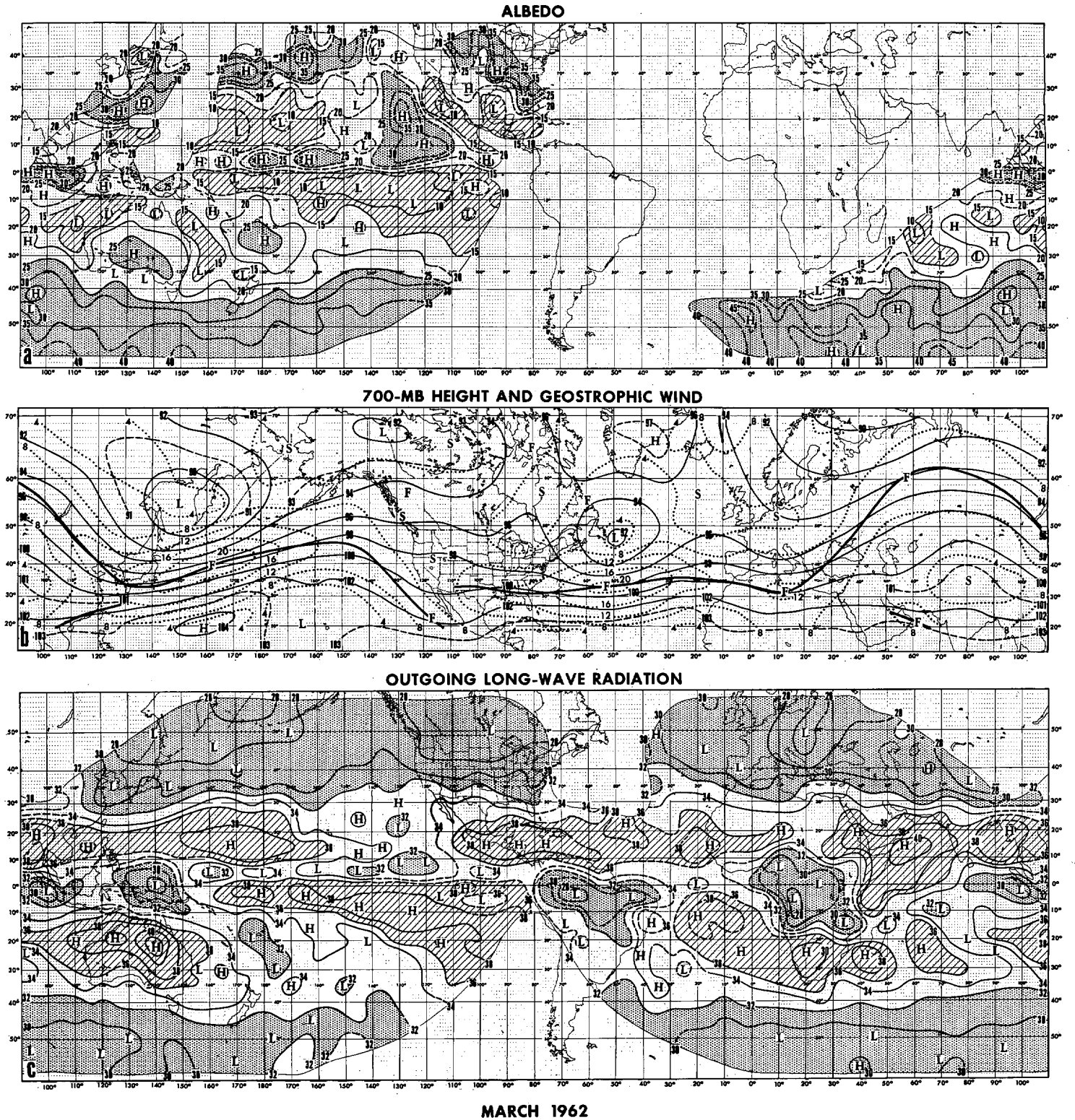


FIGURE 2.—Averages for March 1962 of (a) Albedo. (b) 700-mb. height and geostrophic wind. (c) Outgoing long-wave radiation. See legend to figure 1.

The pronounced south-north gradients of long-wave radiation and albedo located in the lower temperate latitudes generally had strong zonal continuity, but there were some interesting longitudinal variations in the various months. Considering the radiation gradient in

the Northern Hemisphere first, it is apparent that the gradient and the monthly mean 700-mb. wind field were related. The axes of maximum wind speed were generally located north of the strongest south-north radiation gradients. Where the wind speed was high and anticyclonic

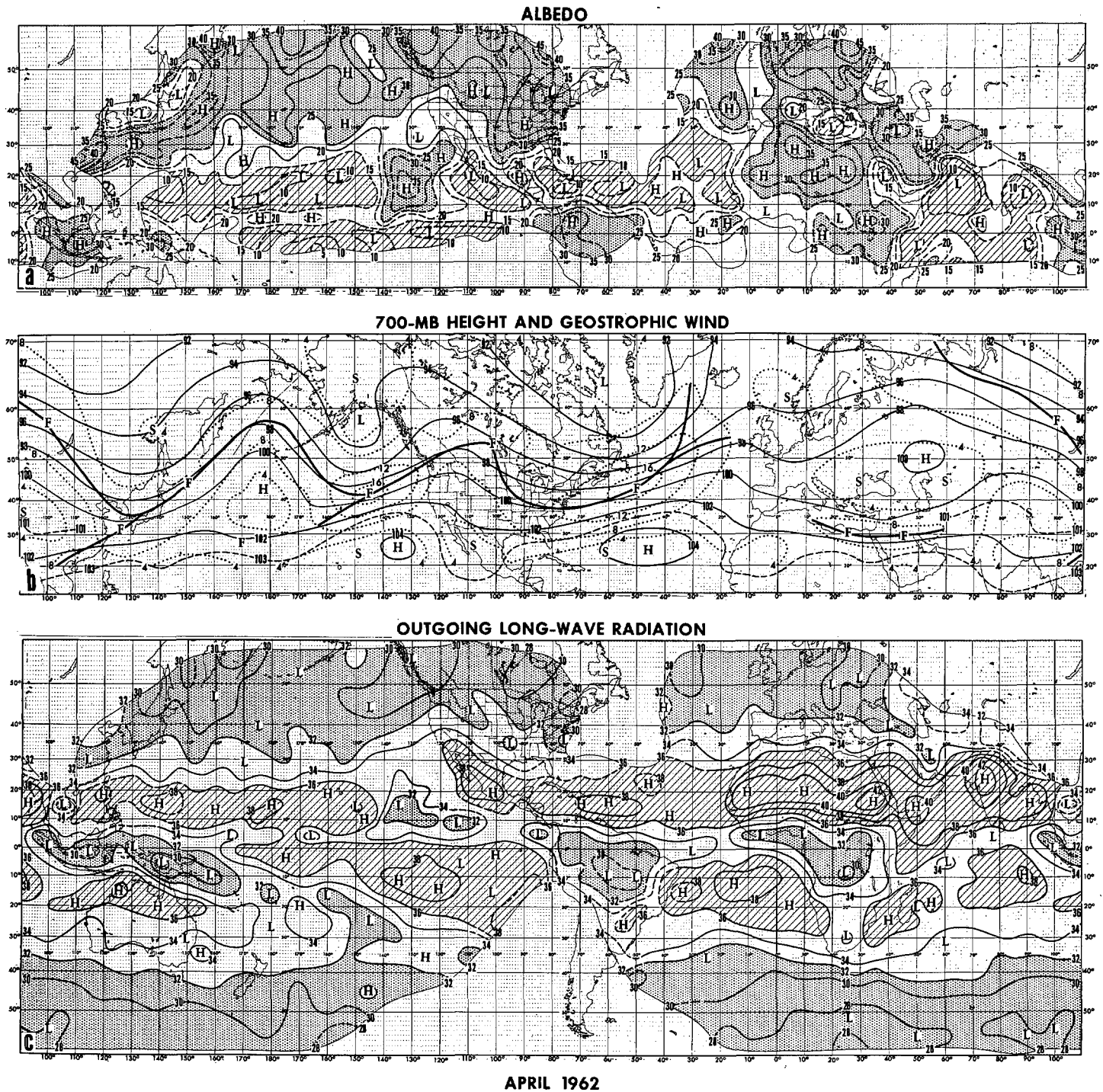


FIGURE 3.—Averages for April 1962 of (a) Albedo. (b) 700-mb. height and geostrophic wind. (c) Outgoing long-wave radiation. See legend to figure 1.

shear strongest, the radiation gradient was strongest. Where the wind speeds were lower or the axis meandered considerably, there were weaker gradients of radiation and they were not so well positioned relative to the wind shear. An example of this may be seen over the Pacific Ocean in figure 1 (b and c) where strong westerlies and strong south-north gradients of long-wave radiation prevailed over the western half of the ocean, whereas

weaker westerlies and a much weaker radiation gradient, associated with a blocking pattern, occurred over the eastern half. In the region of blocking, the south-north gradient of radiation was displaced southward in association with the more southerly branch of the westerlies. This southward intrusion of cloudiness (and associated convergence) and the accompanying less cloudy zone (and associated divergence) to its south were very likely

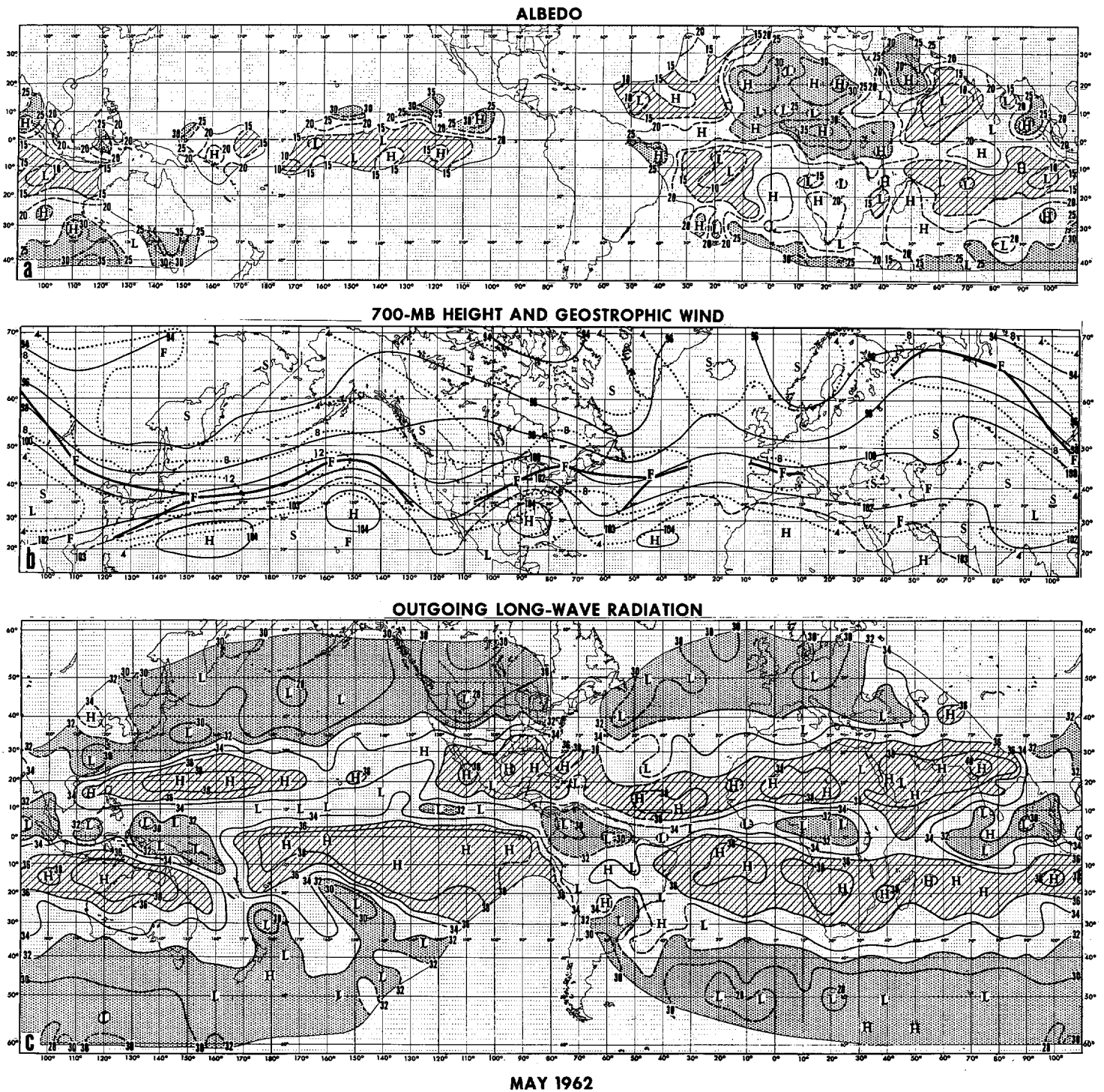


FIGURE 4.—Averages for May 1962 of (a) Albedo. (b) 700-mb. height and geostrophic wind. (c) Outgoing long-wave radiation. See legend to figure 1.

responsible for the virtual absence of activity in the intertropical convergence zone over the central and eastern Pacific during February 1962. The contrast in meridional profiles of radiation for February between the western and eastern Pacific is clearly indicated in figure 7 (135° W. as contrasted with 180° and 135° E.).

Another example of substantial differences in the south-north gradient of radiation in connection with differences

in flow may be found in the western and central North Pacific in March and April (figs. 2, b and c; 3, b and c; and 7 at 135° E. and 180°). In March the south-north gradient was relatively strong, whereas in April it was considerably weaker. This change was associated with a substantial weakening of wind speeds over the area as the strong westerlies in March, associated with the active Asian coastal trough and the strong southwesterly flow

OUTGOING LONG-WAVE RADIATION

FEBRUARY - MAY 1962

LONGITUDE

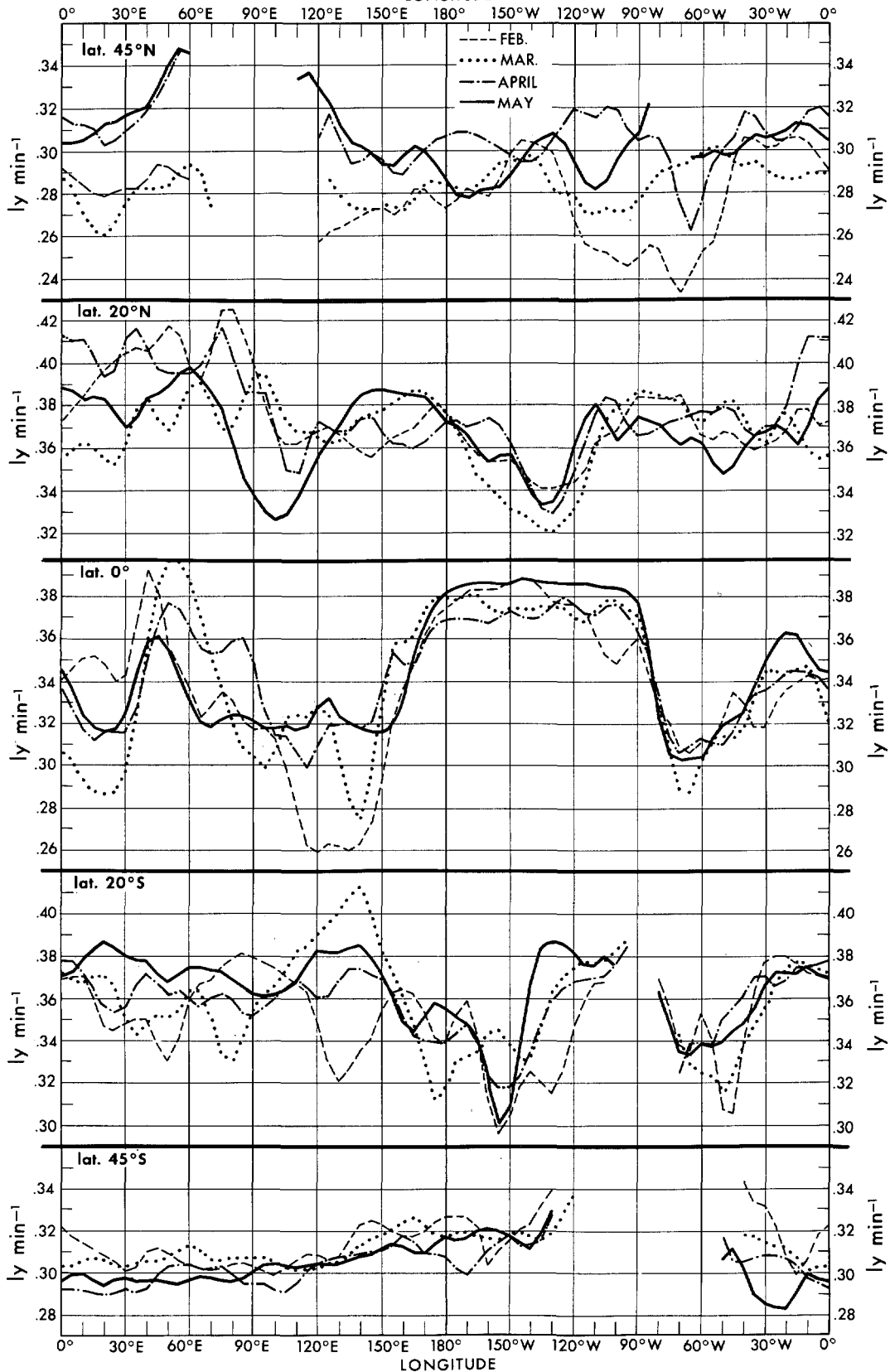


FIGURE 5.—Profiles of outgoing long-wave radiation along selected latitude circles for the months of February-May 1962.

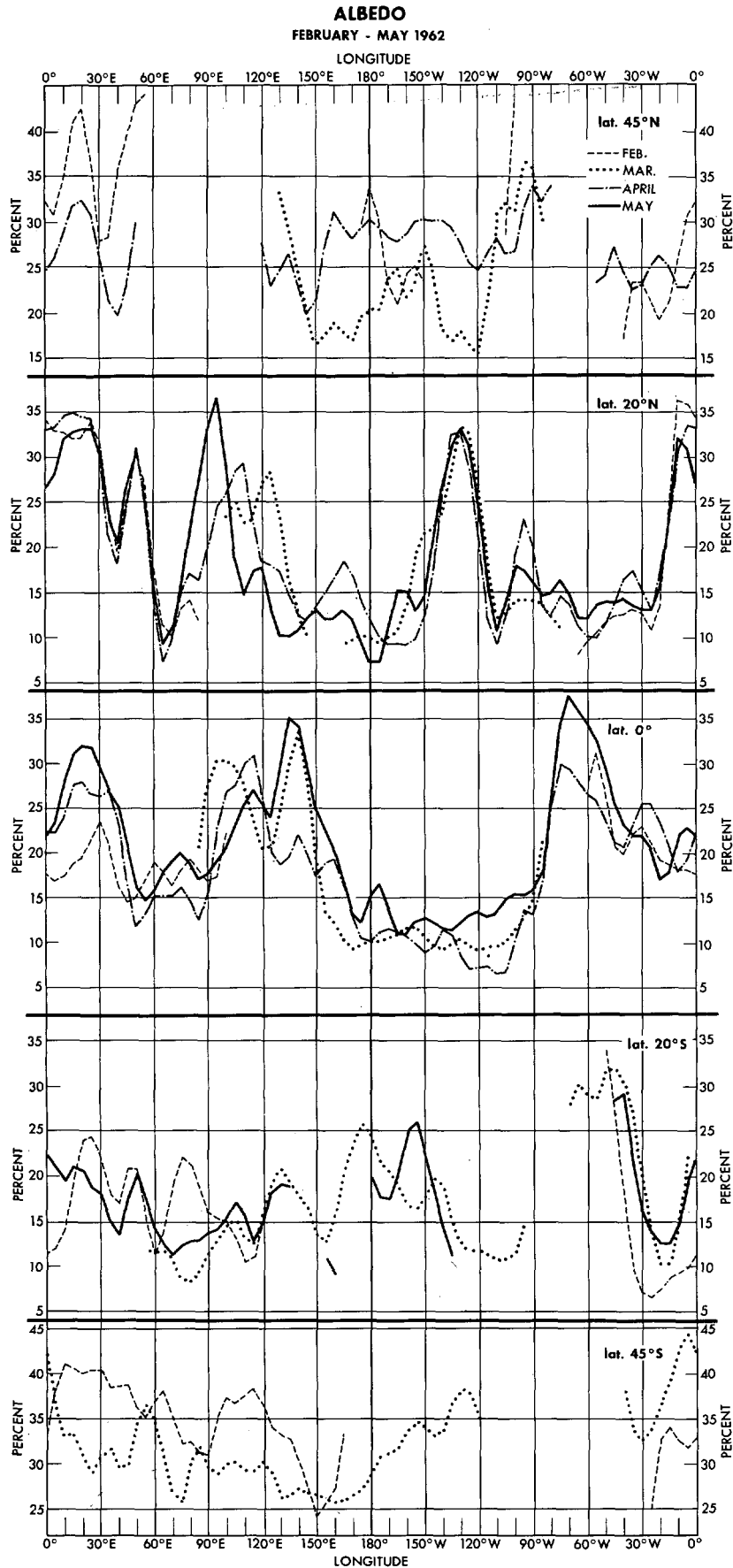


FIGURE 6.—Profiles of albedo along selected latitude circles for the months of February-May 1962.

**OUTGOING LONG-WAVE RADIATION**  
FEBRUARY - MAY 1962

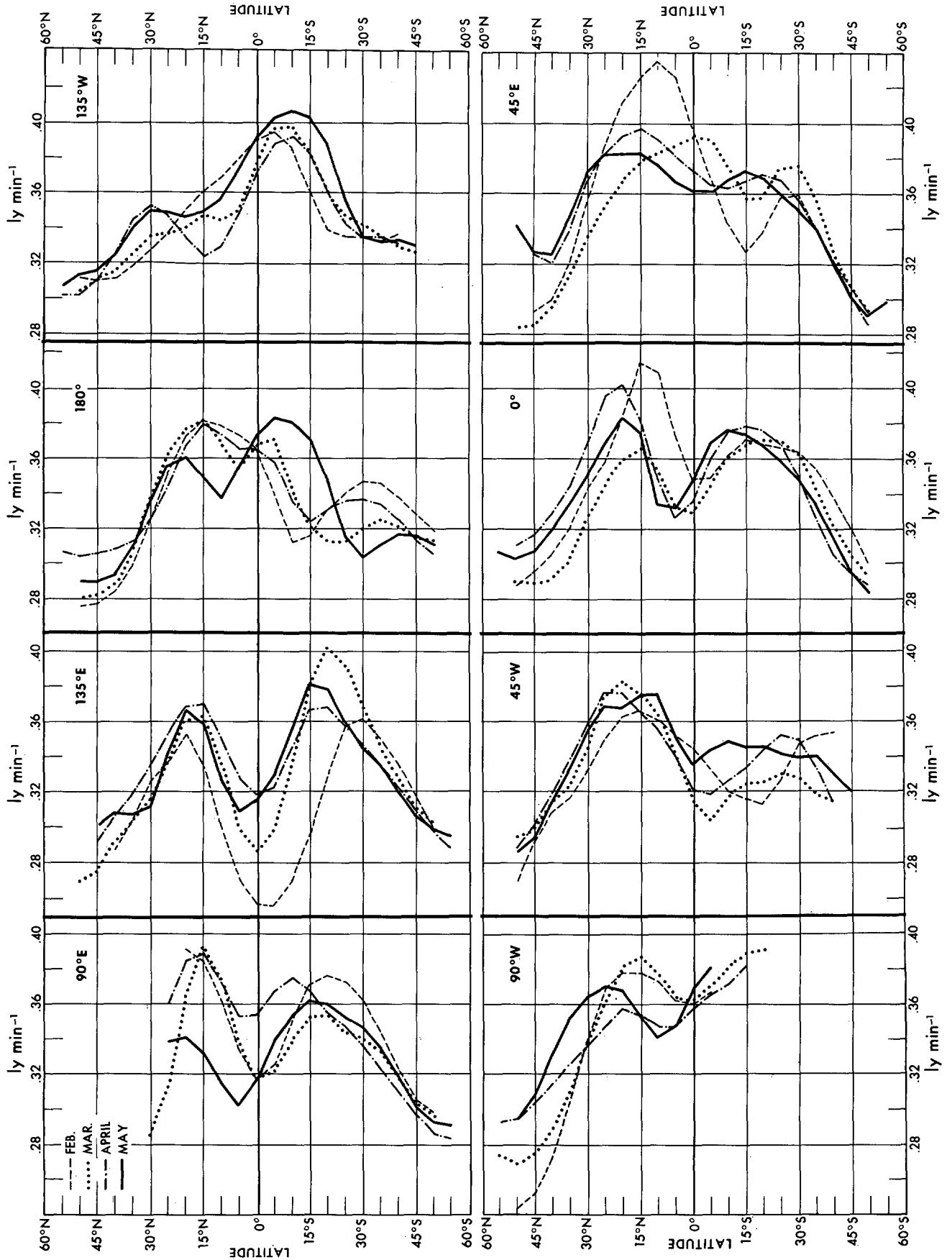


FIGURE 7.—Profiles of outgoing long-wave radiation along selected meridians for the months of February–May 1962.

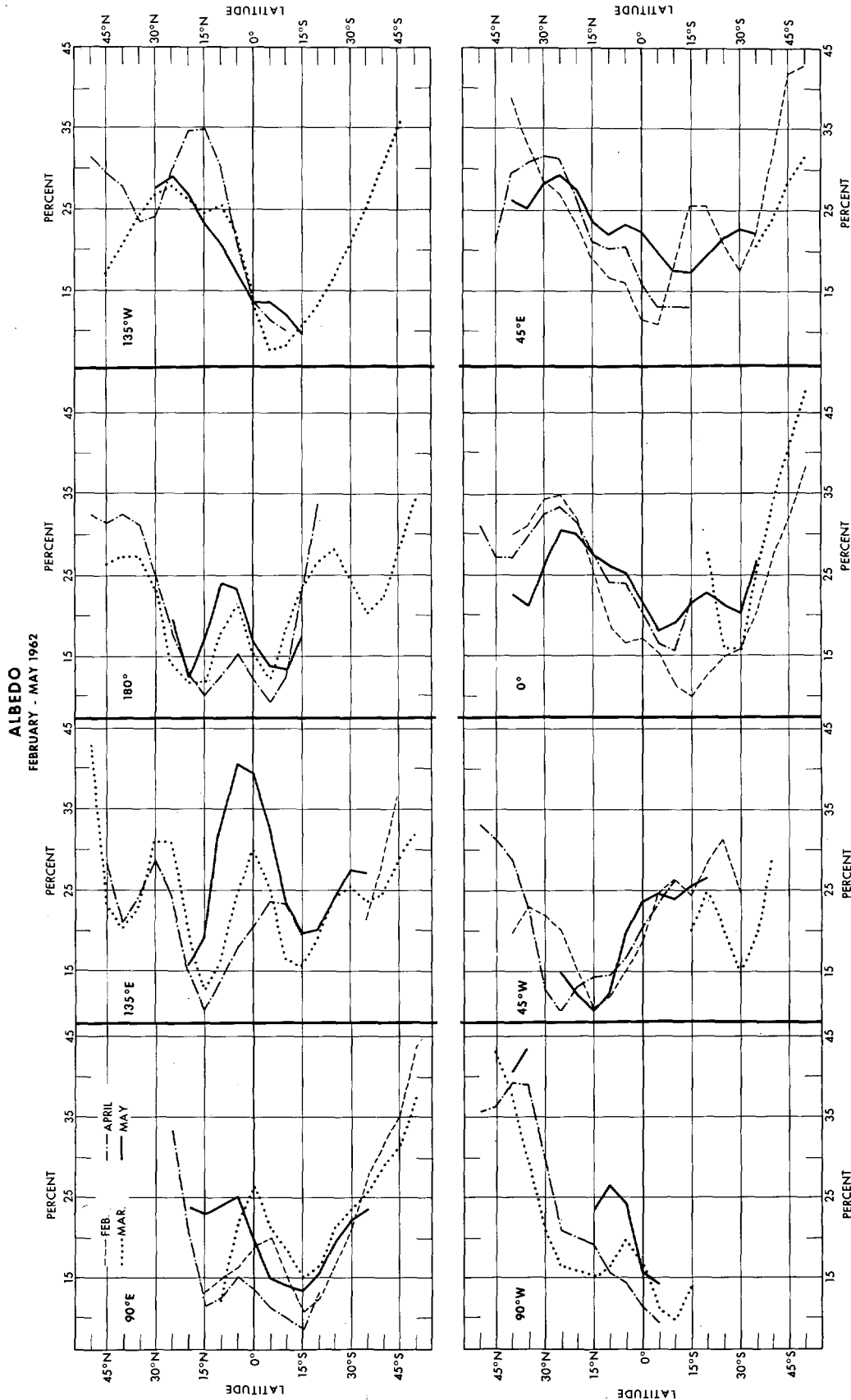


FIGURE 8.—Profiles of albedo along selected meridians for the months of February–May 1962.

to its east, were replaced in April by a weak flow which was split into two branches around a blocking anticyclone over the central Pacific. That this weakening of the radiation gradient was not a seasonal trend is evident from the fact that the radiation gradient strengthened again in May when the westerlies once more increased over the western and central Pacific (fig. 4, b and c).

The corresponding north-south gradient of long-wave radiation between the subtropical and temperate zones of the Southern Hemisphere was generally not so strong as in the Northern Hemisphere (figs. 1c-4c, and 7). Of course, the seasons were reversed, yet the months involved yielded a sampling of both warm and cold season months for each hemisphere. It is evident that the gradient was relatively strong from the eastern Atlantic eastward to the longitude of eastern Australia. Over the central and eastern Pacific this tropical-temperate zone gradient was virtually absent, but a strong gradient was found between the equatorial divergence (or dry) zone and the subtropical convergence zone near 20°-30° S. This may be seen very clearly both on the maps (figs. 1-4) and in the profiles for 135° W. and 180° (fig. 7). The albedo data, when available (figs. 1a, 2a, and 8), essentially showed a similar (but reversed) strong gradient.

Returning to the profiles of long-wave radiation along the meridians (fig. 7), one notes with interest that the profile for 135° W. was most atypical of all longitudes shown for all four months. It will be noted on the maps for each month (figs. 1c-4c) that relatively low radiation values extended northward out of the equatorial zone at this and adjacent longitudes, whereas in almost all other portions of the subtropics values of long-wave radiation tended to be considerably higher. February was already discussed as a blocking case, but the flow patterns in the other months were of a more normal westerly type over the eastern North Pacific. The radiation pattern in February in this area did differ most markedly from the other months, yet all months had the common characteristic of being lower in outgoing radiation and hence of having more middle and high cloudiness than the overwhelming remainder of this latitude belt. Seasonal charts for July-August and September-November of 1963 generally exhibited relatively high outgoing radiation in this region, but December 1963-February 1964 again tended to be low [16]. Thus, at this stage it is known that this radiation minimum is not a permanent year-round feature, but it is not known whether it is a characteristic typical of winter and spring. It is interesting that over the eastern North Atlantic there was no corresponding type of breakthrough of low radiation in the subtropics in any of these months.

One further noteworthy contrast found between long-wave radiation in the Northern and Southern Hemispheres was the very small variability both in longitude and in time at 45° S. in contrast with 45° N. (fig. 5). Most of the larger differences at 45° N., as might be expected, occurred over the continents and most of the changes

TABLE 1.—Correlation coefficients between monthly mean fields of outgoing long-wave radiation and albedo

	Month-(1962)			
	February	March	April	May
Correlation coefficient.....	-0.66	-0.66	-0.58	-0.54
Number of pairs*	(767)	(1032)	(1104)	(1008)

\*Number of 5° latitude-longitude grid points with both types of data.

were in a direction expected from seasonal trends in surface and air temperatures, both of which should substantially affect long-wave radiation. However, even over land there were some non-seasonal monthly differences which could only be attributed to substantial differences in cloudiness (e.g., a minimum of outgoing radiation over the western United States in May as contrasted with a general maximum there in April). Over ocean areas too at 45° N. there was generally more variability both in longitude and in time than at 45° S. It will be noted that the albedo profiles at 45° N. and 45° S. (fig. 6) do not display the same type of relative variability, but the data available for comparison were much more restricted in amount than were the long-wave data.

In the preceding discussion the degrees of similarity between geographical distributions of outgoing long-wave radiation and albedo in the various months were pointed out several times. To express these relationships quantitatively and to provide a convenient compilation of relationships, various linear correlation coefficients between long-wave radiation and albedo have been calculated. Table 1 contains the correlations for the entire area where both quantities were observed in each month (i.e., the correlations between the maps in figs. 1, a and c; 2, a and c; etc.). Tables 2 and 3 list the correlations along selected latitude circles and meridians (i.e., the relationships between the profiles in figs. 5 and 6; 7 and 8).

The correlations are predominantly negative and many may be classified as fair to good.<sup>2</sup> Whether the differences in the correlations between months in tables 1-3 are of any significance is indeterminable from these data, since the sampling variations, both in space and time, were rather sizable from one month to the next. Good negative correlations are generally found at the equator for the zonal variations (table 2) and along a majority of the meridians (table 3). Highest negative correlations are most consistently found at those meridians where oceans or non-desert land areas predominate (e.g., 45° W., 90° W., 135° W., 180°, 135° E., 90° E.). On the other hand, at 0° and 45° E. poor correlations predominate and this can be attributed to the interference of the desert regions, where the albedo and long-wave radiation are positively correlated, with the usual negative correlation that exists in most other regions. With respect to zonal relationships again (table 2), the correlations tend to be poorest at middle latitudes. This may be due to the greater

<sup>2</sup> Classification of correlation coefficients is of course arbitrary. Roughly I am defining an absolute value between 0.4 and 0.7 as fair, greater than 0.7 as good, and less than 0.4 as poor.

TABLE 2.—Correlation coefficients between monthly mean values of outgoing long-wave radiation and albedo along selected latitude circles

Latitude	Month (1962)							
	February		March		April		May	
	All avail- able longi- tudes	Oceans only						
45° N.....	-0.45 (30)		-0.18 (32)		-0.24 (55)	-0.42 (27)		
20° N.....	+ .22 (31)		-.62 (35)	-0.68 (25)	+ .16 (72)	-.87 (43)	-0.25 (72)	-0.72 (43)
0°.....	-.53 (33)	-0.51 (20)	-.92 (38)	-.92 (30)	-.93 (72)	-.89 (48)	-.82 (72)	-.73 (48)
20° S.....	-.89 (35)	-.66 (22)	-.65 (57)	-.78 (42)			-.55 (50)	-.63 (36)
45° S.....	-.61 (40)	-.61 (40)	-.05 (57)	-.03 (56)				

Number in parenthesis shows number of pairs correlated (i.e., number of 5° longitude grid points along the latitude circle with both types of data).

frequency at these latitudes of extensive regions where only low stratus or stratocumulus clouds occur.

In examining the various global monthly charts in figures 1-4 and zonal and meridional profiles in figures 5-8 it is apparent that there is much resemblance of the patterns of both outgoing long-wave radiation and albedo from one month to another. This has been indicated of course by the discussion of broadscale features given earlier. The degree of this persistence in the radiation patterns is also illustrated quantitatively by correlation coefficients between the fields of long-wave radiation and albedo in each of the pairs of months (table 4). In general the planetary patterns of long-wave radiation are rather highly persistent, as indicated by the fair to good positive correlations. The greater persistence of the long-wave radiation as compared with the albedo may be largely due to the more limited areal and temporal coverage of albedo data which cuts down on the contribution of the quasi-permanent, broad zonal belts between 55° N. and 55° S. to the lag correlations.

Despite the general overall resemblance of these radiation patterns, differences between the actual values in these four months were sizable. As an illustration of the extent of changes that occurred in the outgoing long-wave radiation in this period, the differences between February and May 1962 are presented in figure 9. This chart is, of course, composed largely of seasonal types of changes, but there are undoubtedly some features which are more characteristic of the anomalous radiation distributions of February and May 1962. Some noteworthy features of this difference chart are as follows:

(1) Substantial increases of radiation situated over most of the temperate portions of the continents in the Northern Hemisphere and relatively smaller changes (both negative and positive) over the oceans at the same latitudes.

(2) Large falls over Africa, the northern Indian Ocean, and the Bay of Bengal, indicative of the northward shifts of the subtropical anticyclones and the intertropical convergence zone and the development of the monsoonal circulation.

TABLE 3.—Correlation coefficients between monthly mean values of outgoing long-wave radiation and albedo along selected meridians

Longitude	Month (1962)			
	February	March	April	May
0°.....	-0.49 (19)		+0.05 (14)	+0.05 (16)
45° W.....	-.74 (15)		-.95 (13)	-.94 (10)
90° W.....		-0.96 (13)	-.87 (12)	
135° W.....		-.75 (19)	-.88 (13)	-.83 (11)
180°.....		-.87 (20)	-.88 (15)	-.90 (10)
135° E.....		-.61 (21)	-.62 (13)	-.94 (12)
90° E.....	-.80 (14)	-.95 (13)	-.14 (10)	-.71 (12)
45° E.....	-.75 (19)		-.20 (13)	+ .06 (16)

Number in parenthesis shows number of pairs correlated (i.e., number of 5° latitude grid points along the meridian with both types of data).

TABLE 4.—Lag correlations of monthly mean fields of outgoing long-wave radiation and albedo in 1962

Quantity	One-Month Lag			Two-Month Lag		Three-Month Lag
	Feb.- Mar.	Mar.- Apr.	Apr.- May	Feb.- Apr.	Mar.- May	Feb.- May
Long-Wave Radiation..	+0.76 (1473)	+0.78 (1503)	+0.81 (1538)	+0.74 (1477)	+0.73 (1496)	+0.65 (1483)
Albedo.....	+ .59 (409)	+ .53 (636)	+ .54 (821)	+ .63 (508)	+ .40 (654)	+ .48 (587)

Number in parenthesis shows number of pairs correlated (i.e., number of 5° latitude-longitude grid points with both types of data).

(3) Moderately large falls over the Caribbean, Central America, and the central subtropical North Pacific, also basically associated with the northward shift of the subtropical anticyclones and the intertropical convergence zone.

(4) Large rises over subtropical portions of South Africa and South America and over Indonesia, representing the changes to the drier season that accompany the seasonal shift in the intertropical convergence zone.

(5) General falls through much of the temperate zone

**DIFFERENCE IN OUTGOING LONG-WAVE RADIATION**  
FEBRUARY 1962 TO MAY 1962

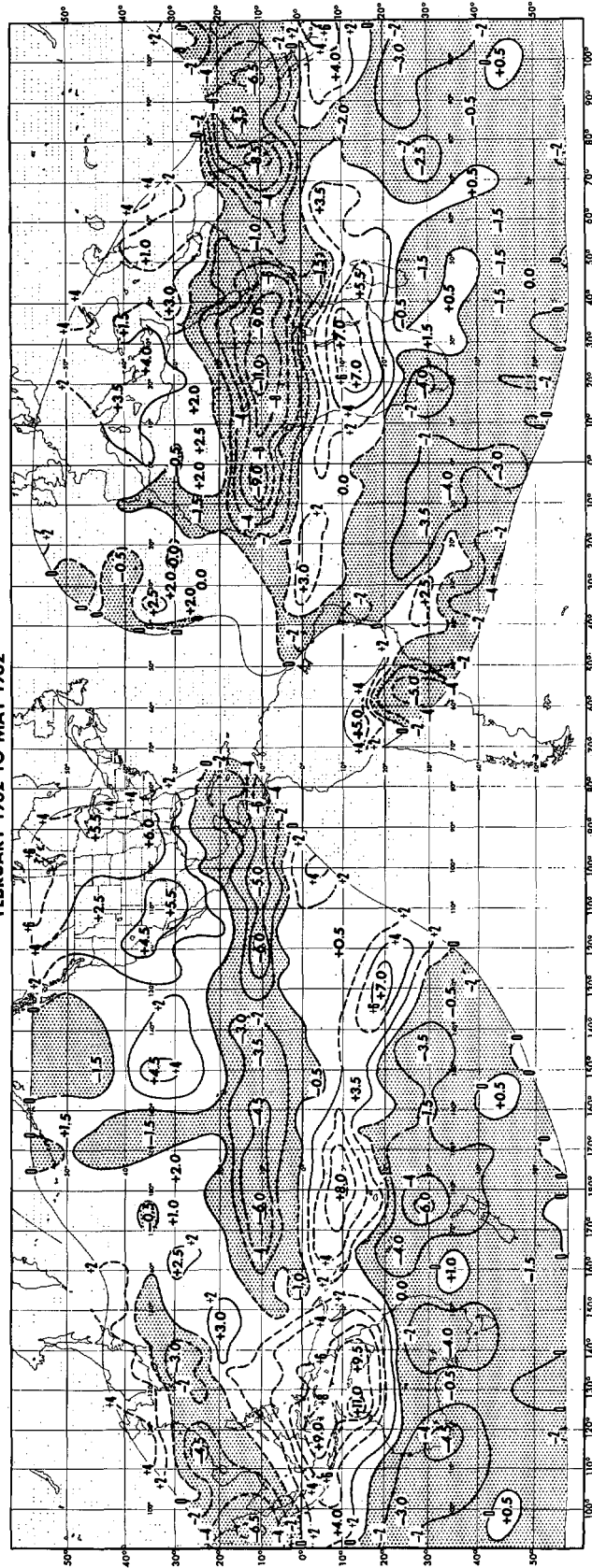


FIGURE 9.—Difference in outgoing long-wave radiation between February and May 1962 (fig. 1c subtracted from fig. 4c). Isopleths and maxima and minima are labeled in hundredths of  $\text{ly. min.}^{-1}$  and are drawn at intervals of  $0.02 \text{ ly. min.}^{-1}$ . Areas with negative differences are stippled. Isopleths are dashed in regions with data on less than one-third of the days in either month and no analysis is shown where data were available on less than one-tenth of the days in either month.

of the Southern Hemisphere, particularly over Australia and across the South Atlantic.

#### 4. COMPARISON OF OUTGOING LONG-WAVE RADIATION DATA FOR THE SAME MONTHS OF TWO DIFFERENT YEARS

Preparation of daily composite values of TIROS VII radiation data through late winter and early spring of 1964 has allowed for construction of monthly mean charts of outgoing long-wave radiation for the months of February and March 1964. Comparison of these radiation charts and the corresponding monthly mean 700-mb. flow patterns (figs. 10 and 11) with the data for February and March 1962 (figs. 1 and 2) provides some very interesting information about the type of variability that can be expected in the radiation data in a given month from one year to another. To facilitate this comparison, charts showing changes in long-wave radiation and 700-mb. height from February and March 1962 to 1964, respectively, are presented in figures 12 and 13.

Since the radiation data for these two years are from two different satellite instruments, neither of which had any check on calibration after launch, one must be cautious in attaching much significance to precise absolute differences in radiation. As mentioned earlier, degradation corrections have been applied to the 1962 data, but not to the 1964 data. Since an overall negative bias was found in the original differences between figures 10 and 1 (February) and 11 and 2 (March), the 1964 data apparently do need some positive correction relative to the corrected 1962 data. Comparison of overall weighted averages of zonal mean data for each chart (approximately 55° N. to 55° S.) showed that the average differences were about  $-0.01 \text{ ly. min.}^{-1}$  for February and  $-0.02 \text{ ly. min.}^{-1}$  for March. To provide difference charts having little overall bias, additive constants of 0.01 and 0.02  $\text{ly. min.}^{-1}$  were applied to the original differences for February and March, respectively. Thus, strictly for purposes of comparison, it has been assumed that the average long-wave radiation over the area covered by the differences did not vary between 1962 and 1964. Incidentally, if the correction factors proposed by Staff Members, NASA [11, 12, 13] had been applied to the 1964 data, the average difference in each month would have been about  $+0.02 \text{ ly. min.}^{-1}$ , i.e., the corrected values appear to be too large relative to the 1962 data. Of course, it is possible that such overall average changes in radiation could occur from one year to another, but since profiles of zonal mean values show a difference of the same sign at almost all latitudes it is likely that an overall positive (or negative) change is more representative of instrumental errors than of a real difference in radiation.

The adjusted differences between the fields of long-wave radiation in each of the two pairs of like months (figs. 12b and 13b) appear to be quite reasonable. Obviously there are many small details in these difference patterns that

may have little meaning in view of the data difficulties, but the coherence of the patterns over large areas is indicative of realistic variations in radiation. It will be noted that the average (absolute) differences over the entire area are about 5 percent of the monthly mean values of radiation and that maximum differences range up to about 30 percent of the mean values.

For the two Februarys the relationships between the radiation differences and the height differences (over the Northern Hemisphere north of 15° N.) are especially close (figs. 1, 10, and 12). Notable in this regard is the area of the eastern North Pacific and the western United States, where the replacement of a strong blocking regime in February 1962 (mentioned earlier) by a more simple sinusoidal type of wave pattern of pronounced amplitude in February 1964 was accompanied by substantial changes in many features of the radiation pattern. Among these were (1) decreases in long-wave radiation over the Gulf of Alaska and northeastern Pacific, where strong southwesterly flow (presumably with more major cloudiness) in 1964 replaced strongly anticyclonic flow (with lesser cloudiness) in 1962; (2) rises in long-wave radiation across middle latitudes between the central Pacific and the central United States, where anticyclonic flow (with fewer clouds) in 1964 replaced the southerly branch of the split westerlies with its accompanying fronts and cyclones (more cloudiness) in 1962; and (3) decreases in long-wave radiation in the subtropical and tropical regions of the eastern Pacific, where increased major cloudiness south of the strong mid-latitude ridge in 1964 apparently replaced lesser cloudiness on the south side of the low-latitude westerlies in 1962. In regard to one aspect of this last difference, the pronounced minimum of long-wave radiation centered near 20° N., 130° W. in February 1964 (fig. 10b) even suggests that a mean low-latitude trough existed to the west of this area (at about 135°–140° W.). Even if such a trough existed, it would not necessarily be revealed in the contour pattern of figure 10a because of the sparsity of pressure-height data in this region. It is also possible of course that the low values of radiation were associated mainly with clouds in the upper troposphere which might indicate a trough at higher levels (e.g., 200 mb.).

Another point of interest in connection with the changes in radiation over the central and eastern Pacific (fig. 12) is that the succession of alternating negative and positive differences north of the equator continues on southward with positive values between about 10° and 20° S. and negative values near 30° S. This is illustrated more explicitly in figure 14 which shows meridional profiles of the differences in long-wave radiation and zonal wind speed averaged between longitudes 125° W. and 160° W. Note that the north-south wavelength of this difference pattern is about 40° to 50° of latitude and that there is a similar spacing (as far as can be seen) in the zonal wind differences. This whole series of changes seems to be in the direction of accentuating the type of meridional

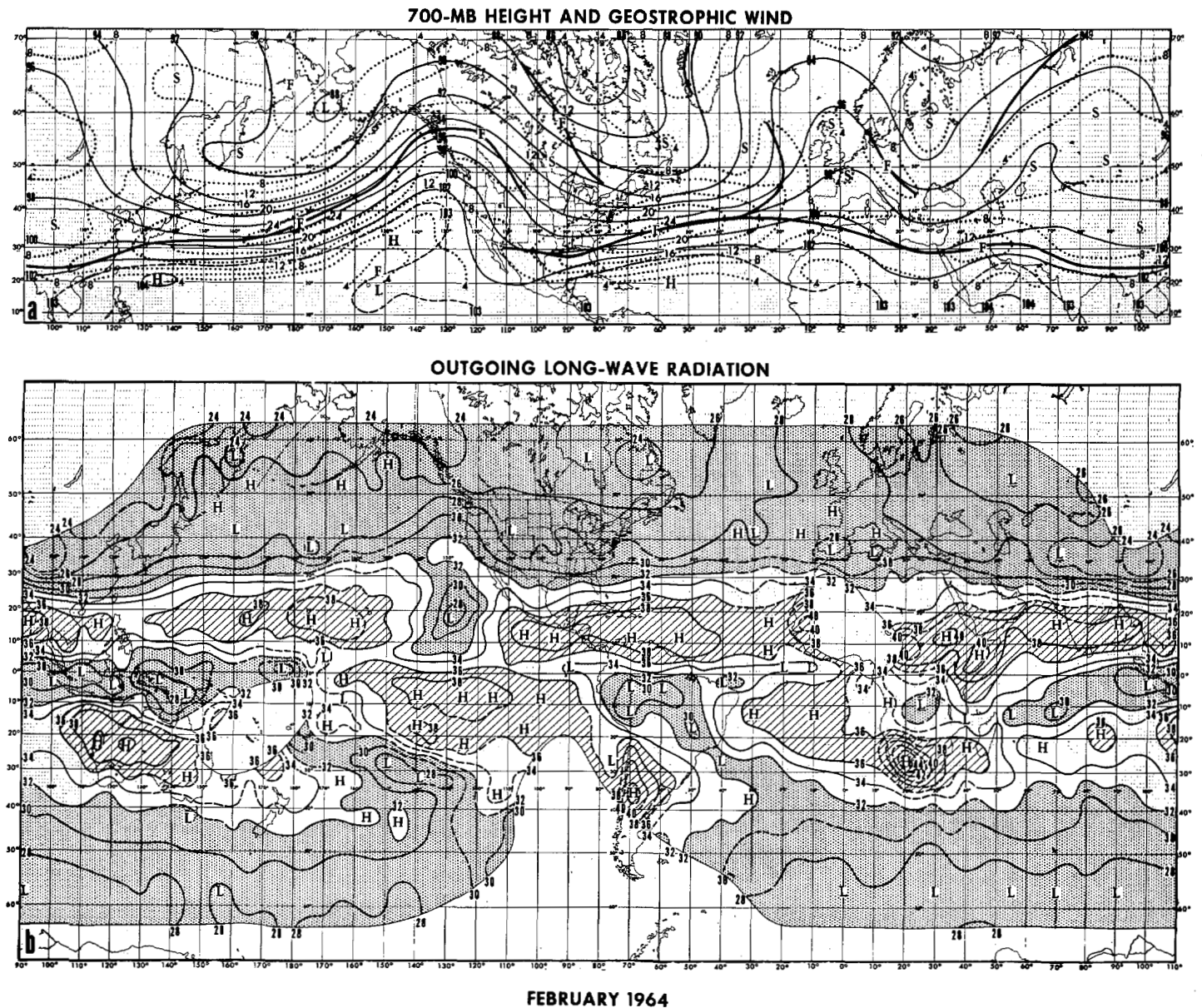


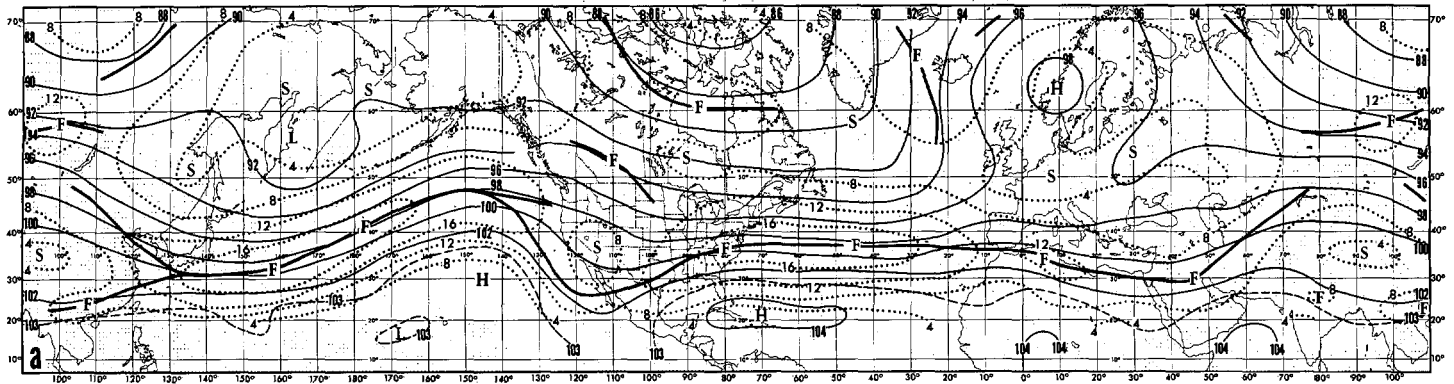
FIGURE 10.—Averages for February 1964 of (a) 700-mb. height and geostrophic wind. (b) Outgoing long-wave radiation. See legend to figure 1.

profile of radiation for the region that is more characteristic of the three other months of 1962 illustrated here. The profiles for the two Februaries, averaged for  $125^{\circ}$  W. to  $160^{\circ}$  W., are shown in figure 15 and these may be compared with the profiles for February-May 1962 at  $135^{\circ}$  W. in figure 7. The difference is reasonable if one considers the relative nature of the flow patterns for the two Februaries. In February 1964 the ridge over the west coast of North America was near its normal longitudinal position, but stronger than normal (fig. 1b). On the other hand, in February 1962 the flow pattern was more distorted from the normal with respect to the longitudinal position of the ridge in the eastern Pacific and to the low-latitude band of westerlies between  $20^{\circ}$  and  $40^{\circ}$  N. (fig. 10a).

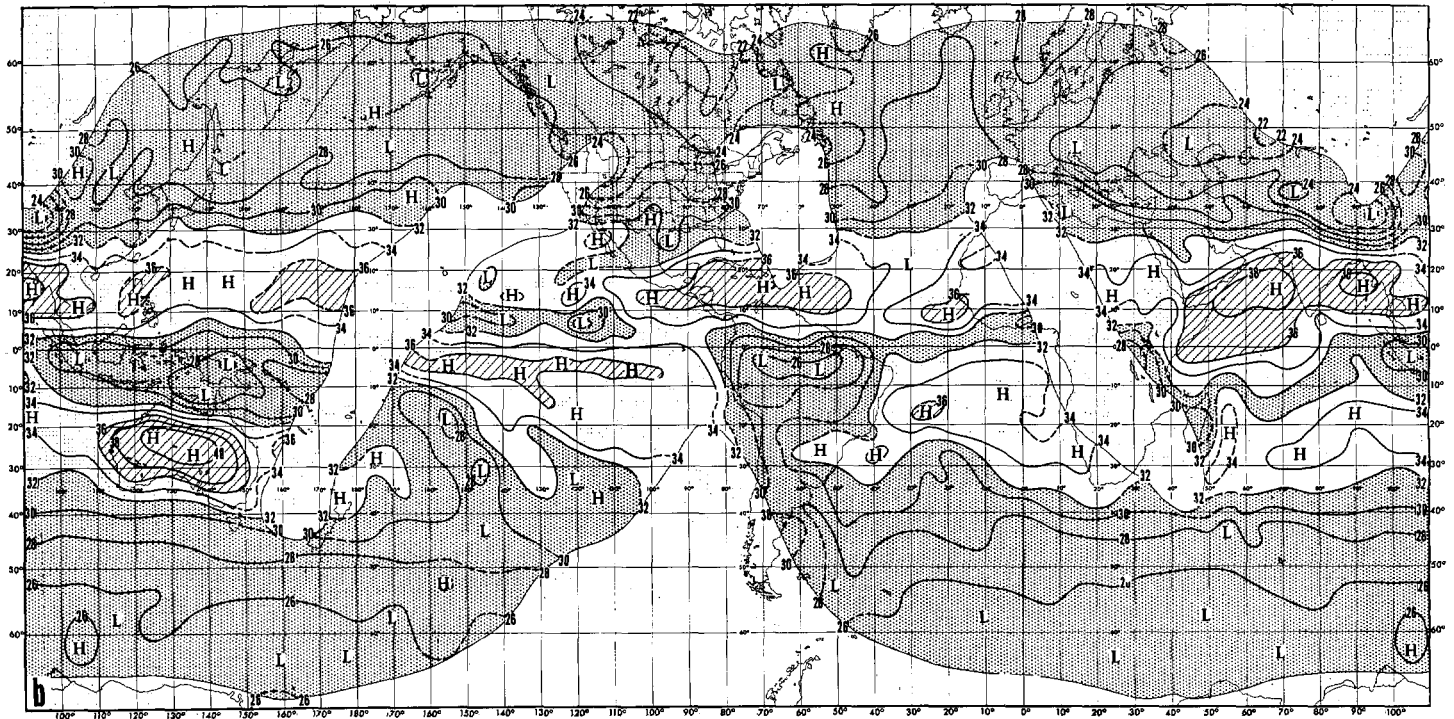
The zonal wind profiles for the two Februaries (fig. 15) also portray some of this contrast clearly. It appears then that a pronounced blocking pattern imposes highly abnormal radiation and cloudiness fields, not only poleward from the subtropics, but also into equatorial regions where the intertropical convergence zone may be suppressed. It is possible furthermore that the essential absence of the latter (figs. 1 and 15) may account for the more equatorward location of the convergence zone in the eastern South Pacific (i.e., near  $20^{\circ}$  S. in February 1962 vs.  $30^{\circ}$  S. in February 1964 as shown in fig. 15), presuming that there is a certain preferred wavelength in the meridional direction.

Such extensive meridional shifts in convergence-

700-MB HEIGHT AND GEOSTROPHIC WIND



OUTGOING LONG-WAVE RADIATION



MARCH 1964

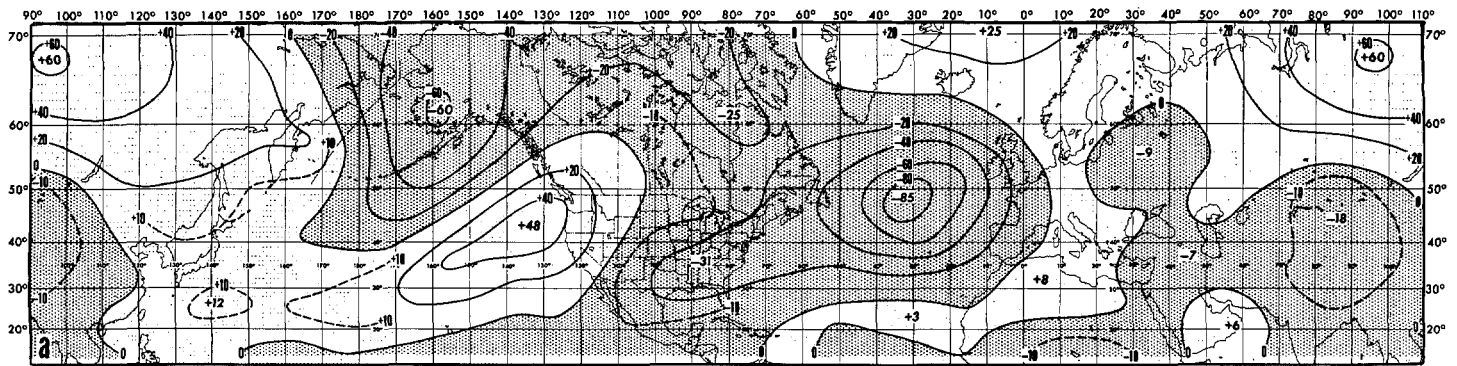
FIGURE 11.—Averages for March 1964 of (a) 700-mb. height and geostrophic wind. (b) Outgoing long-wave radiation. See legend to figure 1.

divergence patterns extending from the Northern to the Southern Hemisphere are similar to differences in circulation and precipitation patterns over the Americas in two different Januarys as pointed out by Namias [5]. This is clearly shown in figure 16 where the meridional profile of differences in percentage of normal precipitation for the two Januarys studied by Namias is given. These differences were taken in the same direction as for the two Februarys, i.e., the changes are from the month with lower-latitude westerlies over North America (January 1958) to the one with westerlies farther northward over North America (January 1950). Thus the zones of negative values which signify decreased precipitation in January 1950 as compared with January 1958, are

analogous to the maxima in figure 14 which signify decreased cloudiness in February 1964 as compared with February 1962. Conversely the maxima in figure 16 essentially correspond to the minima in figure 14. Thus, in the case studied by Namias, there was a meridional pattern of differences in convergence-divergence similar to that for the February 1962-1964 case in the eastern Pacific. In the case studied by Namias the wavelength of the difference pattern was shorter—about 25° to 30° of latitude as compared with 40°-50° of latitude for the February case. Incidentally in Namias' case there seemed to be a general displacement of all characteristic features of the profile southward when the westerlies over North America were farther to the south. In the case in the eastern Pacific

## DIFFERENCE IN 700-MB HEIGHT

FEBRUARY 1962 TO FEBRUARY 1964



## DIFFERENCE IN OUTGOING LONG-WAVE RADIATION

FEBRUARY 1962 TO FEBRUARY 1964

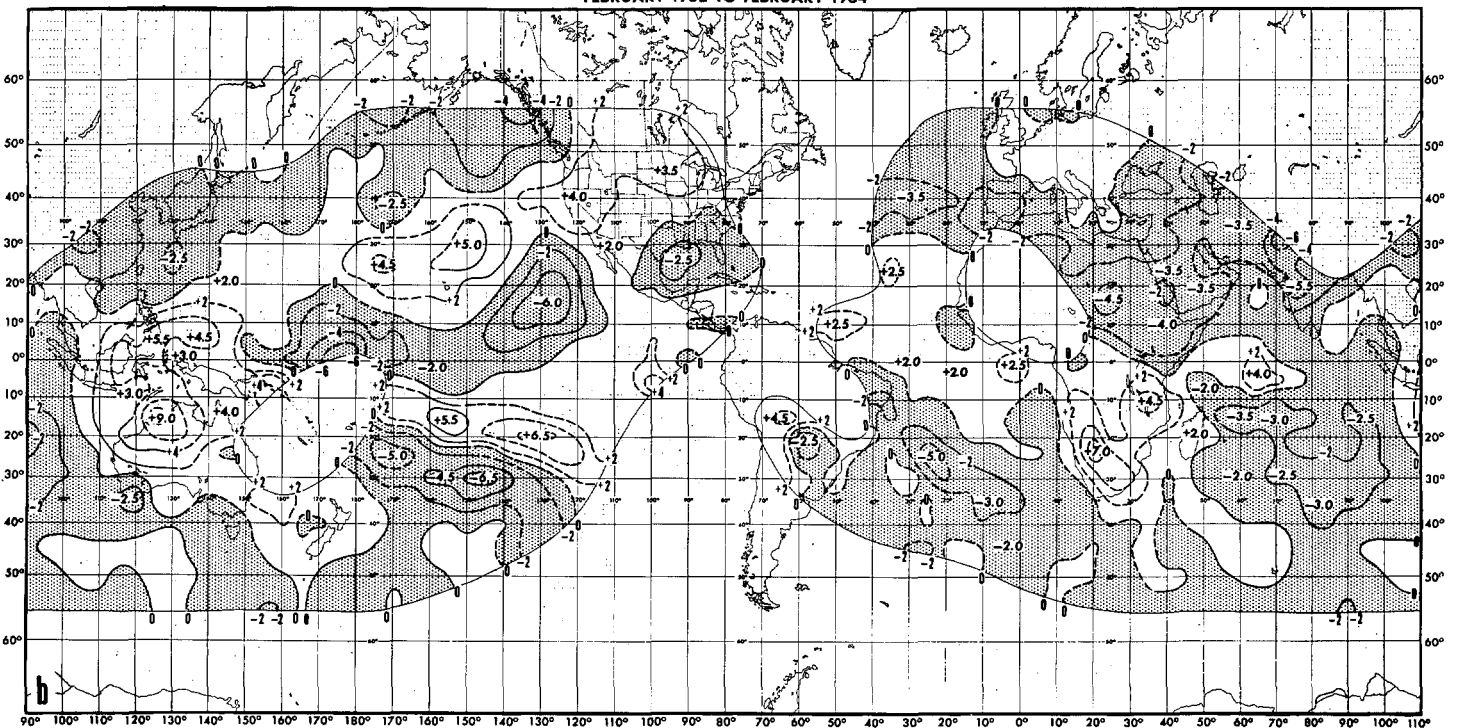


FIGURE 12.—Difference between February 1962 and February 1964 (figs. 1b and 1c subtracted from figs. 10a and 10b, respectively) in (a) 700-mb. height, (b) outgoing long-wave radiation. Isopleths and maxima and minima of 700-mb. height difference are labeled in tens of feet and are drawn at intervals of 200 ft. (solid) with some intermediate 100-ft. isopleths (dashed). Areas with negative height differences are stippled. For the radiation differences see legend to figure 9, except that all values were increased by  $0.01 \text{ ly. min.}^{-1}$  to force the average difference over the area of data to be nearly zero. Also, only centers with absolute values  $0.02 \text{ ly. min.}^{-1}$  or more are labeled.

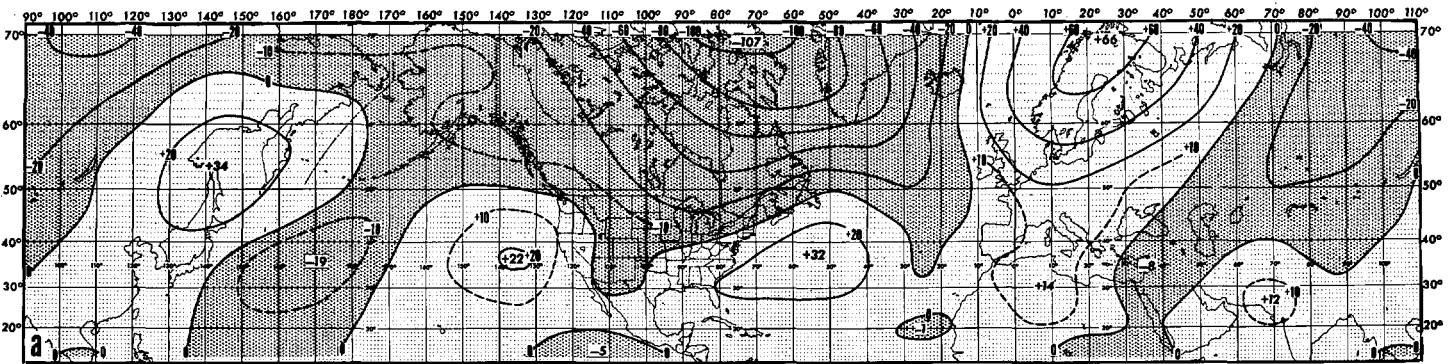
treated here a notable difference was the absence of the minimum of radiation at the normal position of the intertropical convergence and the more northward position of the next minimum south of the equator.

Other February radiation differences over the Northern Hemisphere showing logical relationships to the flow (fig. 12) are (1) negative values over the Gulf of Mexico associated with increased cyclonic flow ahead of the trough in February 1964 (fig. 10a); (2) negative values over the central and eastern Atlantic in middle latitudes ( $35^{\circ}$ – $50^{\circ}$  N.) associated with the very large negative height differ-

ences over the Atlantic (strong cyclonic westerly flow in 1964 as shown in fig. 10a as compared with weak anticyclonic flow in 1962 as shown in fig. 1b); and (3) negative values over much of southern Asia where the lower-latitude westerly belt was stronger in 1964 as evidenced by the negative height differences centered between latitudes  $35^{\circ}$  and  $45^{\circ}$  N.

Many of the areas of larger radiation difference in the Southern Hemisphere (fig. 12b) have extensive meridional orientation between middle latitudes and equatorial regions. This is very pronounced for the negative values

DIFFERENCE IN 700-MB HEIGHT  
MARCH 1962 TO MARCH 1964



DIFFERENCE IN OUTGOING LONG-WAVE RADIATION  
MARCH 1962 TO MARCH 1964

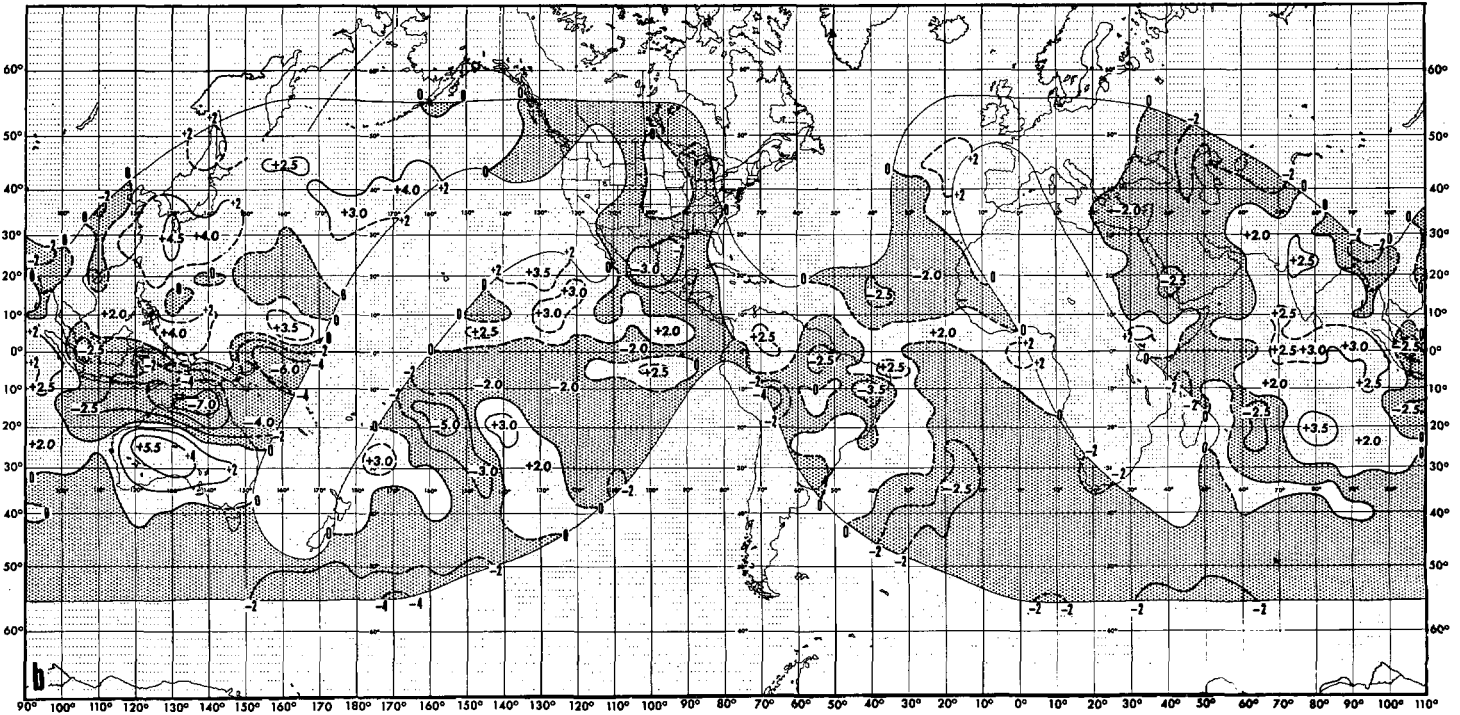


FIGURE 13.—Difference between March 1962 and March 1964 (figs. 2b and 2c subtracted from figs. 11a and 11b, respectively) in (a) 700-mb. height, (b) outgoing long-wave radiation. See legend to figure 12, except that all values of radiation difference were increased by 0.02 ly. min.<sup>-1</sup>

over the South Atlantic and the Indian Oceans and for the positive values over Africa. These differences indicate more meridional orientation of the radiation patterns in these regions in February 1964 and this is evident by comparison of figure 10b with figure 1c. Thus it is likely that the Southern Hemisphere circulation was also more meridional in February 1964.

Over Australia and much of Indonesia positive differences were rather extensive, but not extending as far southward as in the aforementioned regions to the west. These positive values mainly indicate much less latitudinal

breadth to the zone of intertropical convergence activity there in February 1964 as compared with February 1962.

The differences in radiation between March 1962 and March 1964 (fig. 13b) in general show little resemblance to those between February 1962 and 1964 (fig. 12b). (Only in a few areas are radiation difference centers of the same sign found in the same vicinity, such as falls in the Gulf of Mexico, rises over southern Europe, falls near the Black and Caspian Seas.) This is also true for the 700-mb. height differences over the Northern Hemisphere (figs. 13a and 12a). On the average it appears

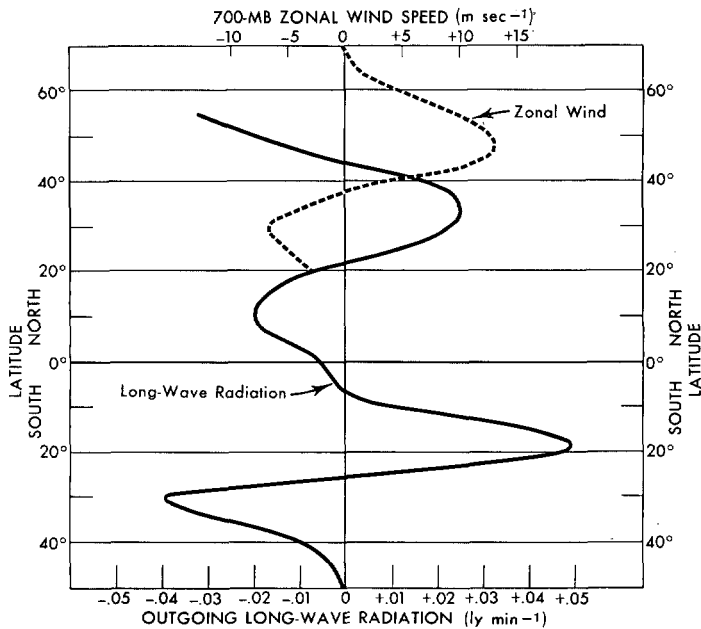


FIGURE 14.—Meridional profiles of differences, averaged over the eastern Pacific (160°–125° W.), in outgoing long-wave radiation and geostrophic zonal wind speed at 700 mb. between February 1962 and February 1964, derived from data illustrated in figure 12.

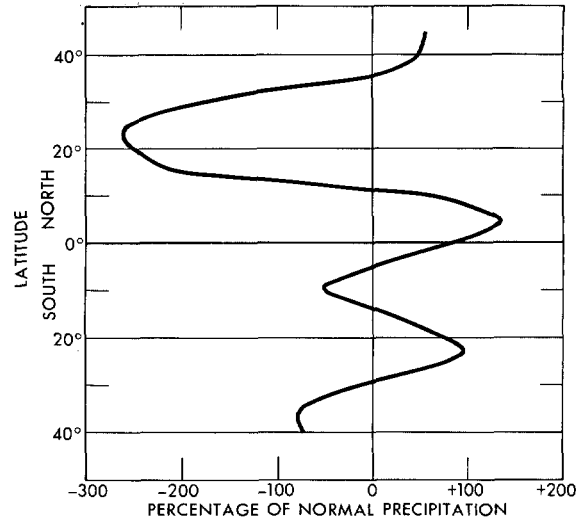


FIGURE 16.—Meridional profile of differences over the Americas in percentage of normal precipitation between January 1958 and January 1950, derived from figure 5 of Namias [5].

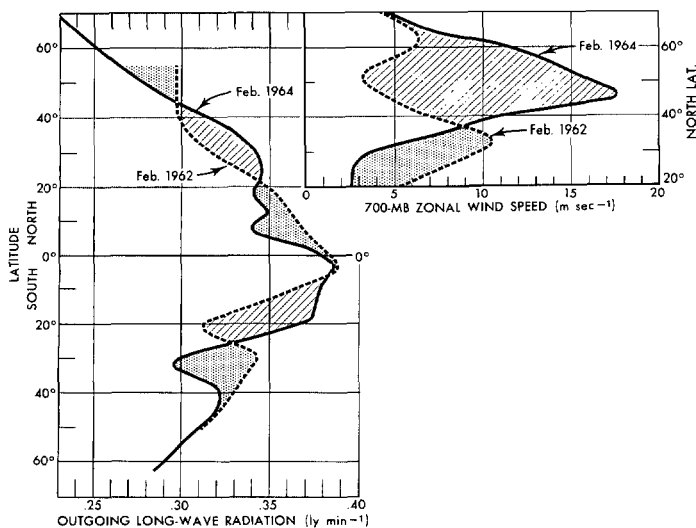


FIGURE 15.—Meridional profiles of outgoing long-wave radiation and geostrophic zonal wind speed at 700 mb. averaged over the eastern Pacific (160°–125° W.) for February 1962 and February 1964, derived from data illustrated in figures 1 and 10. Long-wave radiation values for February 1964 were increased by 0.01  $ly \cdot min^{-1}$  (see legend to fig. 12).

that the March radiation differences over the Northern Hemisphere are somewhat smaller than those for February and this is likewise true of the height differences except at higher latitudes (beyond the northern limit of the radiation data). Over the equatorial regions and the Southern Hemisphere the March radiation differences are generally about as large as those for February.

Relationships between the 700-mb. height changes and the radiation changes for March are generally not as clearcut as for February. Of course, the greater gaps in the radiation data account for this in part since they prohibit a broad view of the radiation differences across the eastern Pacific and the western Atlantic. Also, poorer relationships would be expected when the changes in the height and radiation fields are less definite, particularly since both data fields are subject to errors.

Nevertheless some of the more pronounced differences in radiation for March over the Northern Hemisphere appear to be explicable in terms of differences in the height fields. Note that a reasonable relationship holds over the western Pacific Ocean area where markedly increased long-wave radiation occurred over a large area centered over southern Japan. This increased radiation fits logically with the positive height differences over eastern Asia and the western Pacific (fig. 13a) which signify decreased intensity of the Asian coastal trough in March 1964 (fig. 11a) as compared with March 1962 (fig. 2b). Lowered radiation values over Mexico and the Gulf of Mexico were related to sharpening of low-latitude troughiness over western Mexico from 1962 to 1964 (as indicated by the height rises off both the Pacific

and Atlantic coasts of the United States in fig. 13a). Likewise, negative differences in the North Atlantic off the west coast of Africa and over Saudi Arabia appear to have been related to increased sharpening of low-latitude troughiness. The extensive negative differences in radiation extending from the eastern Mediterranean northeastward to the Black and Caspian Seas and the positive differences over Europe accompanied the extensive changes from a large-scale trough over Europe in March 1962 (fig. 2b) to a large-scale blocking anticyclone in March 1964 (fig. 11a). The farther eastward position of the trough in March 1964 was apparently largely responsible for increased major cloudiness and lower radiation over the Black and Caspian Sea region, although colder air and longer-lasting snow cover in March 1964 may have also contributed to lower radiation values.

The most spectacular differences in long-wave radiation over the equatorial region and the Southern Hemisphere occurred over the central and western Pacific and Australasia (fig. 13b). Negative values extended over a large area from  $0^{\circ}$  to  $20^{\circ}$  S. and from  $105^{\circ}$  E. to at least  $170^{\circ}$  E.; in fact, interpolation across the data gap in the mid-Pacific suggests that these falls connected southeastward with the negative region centered at  $20^{\circ}$  S.,  $155^{\circ}$  W. Positive values to the north (centered near  $5^{\circ}$  N.) and to the south over the southern two-thirds of Australia (and apparently eastward to  $170^{\circ}$  W.) were equally extensive in a zonal direction. It is obvious from these differences and from inspection of the radiation patterns of the two Marches (figs. 2c and 11b) that the intertropical convergence zone in this region was most intense south of the equator in March 1964 and most intense at or north of the equator in March 1962. In general it appears that the latitudinal breadth of the convergence zone was considerably greater in March 1964 and its connection southeastward to the mid-Pacific convergence zone was stronger. The zone of maximum radiation and, by inference, the subtropical anticyclone over Australia were likewise displaced farther southward in March 1964.

There is some suggestion in figure 13b that this pronounced north-south pattern of alternating positive and negative differences extended northward to the area of rises over the western North Pacific which were mentioned earlier. Admittedly the negative differences were not continuous across the region eastward from the northern Philippines, but a definite minimum existed. This whole north-south pattern exhibited a rather well-defined wave pattern with average wavelength of about  $25^{\circ}$  to  $35^{\circ}$  of latitude. In general the character of this zonally oriented pattern of radiation differences resembles the pattern over the central and eastern Pacific for the two Februarys (fig. 12b), except that the average north-south wavelength was larger in the latter case.

In other portions of the Southern Hemisphere the difference pattern for March 1962 to 1964 was neither as well-defined, nor as large-scale, except for the meridionally extensive region of negative differences over the South

Atlantic and predominantly positive differences over the central Indian Ocean from near  $40^{\circ}$  S. northward to India.

## 5. SUMMARY

Characteristics of spatial and temporal variations in monthly averaged outgoing long-wave radiation and albedo have been examined on a global basis with special emphasis on the relationships between the radiation patterns and the mid-tropospheric flow in the Northern Hemisphere and between long-wave radiation and albedo. Albedo and long-wave radiation are inversely correlated on a broad scale, particularly over ocean and non-desert regions. Both quantities show broadscale relationships to the strength and location of features of the wave patterns and the westerlies over the Northern Hemisphere. Although the overall radiation patterns exhibit a moderate degree of persistence from one month to another, differences in the monthly patterns are sizable. Differences in outgoing long-wave radiation for the same month in different years average (on an absolute basis) about 5 percent of the mean values of the radiation and range up to about 30 percent of the mean values. The patterns of these differences in radiation over the Northern Hemisphere are comparable in spatial dimension and bear relation to the differences in the 700-mb. height. The existence of broad zonal belts of differences of alternating sign suggests rather substantial north-south displacements of the radiation pattern and the flow field from one year to another; these extend from the temperate zone of one hemisphere to that of the other. These zonally oriented belts do not extend all the way around the Northern Hemisphere, but are limited to sectors  $60^{\circ}$  to  $90^{\circ}$  of longitude wide. Other parts of the difference patterns are dominated by broad meridional swaths of differences which suggest well organized west-east wave patterns which are nearly in phase over  $40^{\circ}$ - $60^{\circ}$  of latitude extending from temperate to equatorial regions.

## ACKNOWLEDGMENTS

The assistance of Messrs. V. R. Taylor, P. K. Rao, and E. G. Astling in the analysis of monthly mean radiation and circulation maps is very much appreciated. I am also grateful to Messrs. R. Koffler and C. L. Earnest for excellent programing support in compiling and mapping the radiation and other data; to Messrs. J. M. Foard, J. J. Hildebrand, and C. L. Jones for extensive general assistance and some computational work in the preparation of both radiation and other data; and to Mr. L. D. Hatton for his very painstaking work in drafting the figures.

## REFERENCES

1. E. G. Astling and L. H. Horn, "Some Geographical Variations of Terrestrial Radiation Measured by TIROS II," *Journal of Atmospheric Sciences*, vol. 21, No. 1, Jan. 1964, pp. 30-34.
2. W. R. Bandeen, M. Halev, and I. Strange, "A Radiation Climatology in the Visible and Infrared from the TIROS Meteorological Satellites," *NASA Technical Note D-2534*, National Aeronautics and Space Administration, Washington, D.C., June 1965, 30 pp.
3. F. B. House, "The Radiation Balance of the Earth from a

- Satellite," Ph. D. Thesis, Department of Meteorology, The University of Wisconsin, Madison, Wis., 1965, 69 pp.
4. J. H. Lienesch and D. Q. Wark, "Infrared Limb-Darkening of the Earth from Statistical Analysis of TIROS Data," To be published in *Journal of Applied Meteorology*.
  5. J. Namias, "Interactions of Circulation and Weather between Hemispheres," *Monthly Weather Review*, vol. 91, Nos. 10-12, Oct.-Dec. 1963, pp. 482-486.
  6. C. Prabhakara and S. I. Rasool, "Evaluation of TIROS Infrared Data," Proceedings of the *First International Symposium on Rocket and Satellite Meteorology* (Edited by H. Wexler and J. E. Caskey, Jr.), North-Holland Publishing Co., Amsterdam, 1963, pp. 234-246.
  7. P. K. Rao, E. G. Astling, and F. J. Winninghoff, "An Investigation of Degradation Errors in TIROS IV Scanning Radiometer Data and the Determination of Correction Factors," Meteorological Satellite Laboratory Report No. 34, National Environmental Satellite Center, ESSA, 1965, 22 pp.
  8. S. I. Rasool and C. Prabhakara, "Heat Budget of the Southern Hemisphere," *Problems in Atmospheric Circulation*, Garcia and Malone, eds., Spartan Books, Washington, D.C., 1966, pp. 76-92.
  9. I. Ruff, R. Koffler, S. Fritz, J. S. Winston, and P. K. Rao, "Angular Distribution of Solar Radiation Reflected from Clouds as Determined from TIROS IV Radiometer Measurements," ESSA Technical Report NESC-38, National Environmental Satellite Center, ESSA, 1966, 64 pp.
  10. Staff Members, Aeronomy and Meteorology Division, Goddard Space Flight Center, National Aeronautics and Space Administration, *TIROS IV Radiation Data Catalog and Users' Manual*, Goddard Space Flight Center, NASA, Greenbelt, Md., 1963, 250 pp.
  11. Staff Members, Aeronomy and Meteorology Division, Goddard Space Flight Center, National Aeronautics and Space Administration, *TIROS VII Radiation Data Catalog and Users' Manual*, vol. 1, Goddard Space Flight Center, NASA, Greenbelt, Md., 1964, 255 pp.
  12. Staff Members, Aeronomy and Meteorology Division, Goddard Space Flight Center, National Aeronautics and Space Administration, *TIROS VII Radiation Data Catalog and Users' Manual*, vol. 2, Goddard Space Flight Center, NASA, Greenbelt, Md., 1964, 200 pp.
  13. Staff Members, Laboratory for Atmospheric and Biological Sciences, Goddard Space Flight Center, National Aeronautics and Space Administration, *TIROS VII Radiation Data Catalog and Users' Manual*, vol. 3, Goddard Space Flight Center, NASA, Greenbelt, Md., 1965, 269 pp.
  14. Staff Members, Laboratory for Atmospheric and Biological Sciences, Goddard Space Flight Center, National Aeronautics and Space Administration, *TIROS VII Radiation Data Catalog and Users' Manual*, vol. 4, Goddard Space Flight Center, NASA, Greenbelt, Md., 1966, 293 pp.
  15. D. Q. Wark, G. Yamamoto, and J. H. Lienesch, "Methods of Estimating Infrared Flux and Surface Temperature from Meteorological Satellites," *Journal of the Atmospheric Sciences*, vol. 19, No. 5, Sept. 1962, pp. 369-384.
  16. J. S. Winston, "Global Distribution of Cloudiness and Radiation for Seasons as Measured from Weather Satellites," Chap. VII of vol. III (*Climate of the Free Atmosphere*) of *World Survey of Climatology*, Elsevier Publishing Co., Amsterdam, to be published in 1967.
  17. J. S. Winston, "Zonal and Meridional Analysis of 5-Day Averaged Long-Wave Radiation Data from TIROS IV over the Pacific Sector in Relation to the Northern Hemisphere Circulation," to be published in *Journal of Applied Meteorology*, June 1967.
  18. J. S. Winston and P. K. Rao, "Temporal and Spatial Variations in the Planetary-Scale Outgoing Long-Wave Radiation as Derived from TIROS II Measurements," *Monthly Weather Review*, vol. 91, Nos. 10-12, Oct.-Dec. 1963, pp. 641-657.

[Received January 13, 1967; revised March 3, 1967]